Nonlinear Cherenkov radiation at the interface of two different nonlinear media

Xiaohui Zhao,[1,2] Yuanlin Zheng,[1,2] Huaijin Ren,[3] Ning An,[4] Xuewei Deng,[5,6] and Xianfeng Chen[1,2,*]

[1]*State Key Laboratory of Advanced Optical Communication Systems and Networks, Department of Physics and Astronomy, Shanghai Jiao Tong University, 800 Dongchuan Road, Shanghai 200240, China*
[2]*Key Laboratory for Laser plasmas (Ministry of Education), Collaborative Innovation Center of IFSA (CICIFSA), Shanghai Jiao Tong University, 800 Dongchuan Road, Shanghai 200240, China*
[3]*Institute of Applied Electronics, China Academy of Engineering Physics, Mianyang, Sichuan 621900, China*
[4]*Shanghai Institute of Laser Plasma, China Academy of Engineering Physics, Shanghai, 201800 China*
[5]*Laser Fusion Research Center, China Academy of Engineering Physics, Mianyang, Sichuan 621900, China*
[6]*xwdeng@caep.ac.cn*
[*]*xfchen@sjtu.edu.cn*

Abstract: We discuss the nonlinear response due to the spatial modulation of the second-order susceptibility at the interface between two nonlinear media, and experimentally demonstrate that the nonlinear Cherenkov radiation is enhanced by the interface of two nonlinear crystals with a large disparity in $\chi^{(2)}$. In our experiment, the intensity of the nonlinear Cherenkov radiation generated at the nonlinear interface was approximately 4 to 10 times that at the crystal boundary. This result suggests potential applications to efficient frequency conversion.

OCIS codes: (190.0190) Nonlinear optics; (190.4350) Nonlinear optics at surfaces; (190.2620) Harmonic generation and mixing.

References and links

1. A. Zembrod, H. Puell, and J. Giordmaine, "Surface radiation from non-linear optical polarisation," Opt. Quantum Electron. **1**, 64 (1969).
2. H. Ren, X. Deng, Y. Zheng, N. An, and X. Chen, "Nonlinear Cherenkov radiation in an anomalous dispersive medium," Phys. Rev. Lett. **108**, 223901 (2012).
3. Y. Zhang, Z. Gao, Z. Qi, S. Zhu, and N. Ming, "Nonlinear Čerenkov radiation in nonlinear photonic crystal waveguides," Phys. Rev. Lett. **100**, 163904 (2008).
4. C. Chen, J. Lu, Y. Liu, X. Hu, L. Zhao, Y. Zhang, G. Zhao, Y. Yuan, and S. Zhu, "Cerenkov third-harmonic generation via cascaded $\chi^{(2)}$ processes in a periodic-poled $LiTaO_3$ waveguide," Opt. Lett. **36**, 1227 (2011).
5. Y. Sheng, W. Wang, R. Shiloh, V. Roppo, Y. Kong, A. Arie, and W. Krolikowski, "Čerenkov third-harmonic generation in 2 nonlinear photonic crystal," Appl. Phys. Lett. **98**, 241114 (2011).
6. N. An, H. Ren, Y. Zheng, X. Deng, and X. Chen, "Cherenkov high-order harmonic generation by multistep cascading in $\chi^{(2)}$ nonlinear photonic crystal," Appl. Phys. Lett. **100**, 221103 (2012).
7. N. An, Y. Zheng, H. Ren, X. Zhao, X. Deng, and X. Chen, "Normal, degenerated, and anomalous-dispersion-like Cerenkov sum-frequency generation in one nonlinear medium," Photonics Res. **3**, 106 (2015).
8. C. Chen, X. Hu, Y. Xu, P. Xu, G. Zhao, and S. Zhu, "Čerenkov difference frequency generation in a two-dimensional nonlinear photonic crystal," Appl. Phys. Lett. **101**, 071113 (2012).
9. H. Ren, X. Deng, Y. Zheng, N. An, and X. Chen, "Surface phase-matched harmonic enhancement in a bulk anomalous dispersion medium," Appl. Phys. Lett. **103**, 021110 (2013).
10. W. Shi, Y. J. Ding, N. Fernelius, and K. Vodopyanov, "Efficient, tunable, and coherent 0.18–5.27-THz source based on GaSe crystal," Opt. Lett. **27**, 1454 (2002).
11. A. Aleksandrovsky, A. Vyunishev, A. Zaitsev, A. Ikonnikov, and G. Pospelov, "Ultrashort pulses characterization by nonlinear diffraction from virtual beam," Appl. Phys. Lett. **98**, 061104 (2011).
12. Y. Sheng, A. Best, H.-J. Butt, W. Krolikowski, A. Arie, and K. Koynov, "Three-dimensional ferroelectric domain visualization by Čerenkov-type second harmonic generation," Opt. Express **18**, 16539 (2010).

#263353 Received 19 Apr 2016; revised 26 May 2016; accepted 30 May 2016; published 3 Jun 2016

13. X. Zhao, Y. Zheng, H. Ren, N. An, and X. Chen, "Cherenkov second-harmonic Talbot effect in one-dimension nonlinear photonic crystal," Opt. Lett. **39**, 5885 (2014).
14. S. M. Saltiel, Y. Sheng, N. Voloch-Bloch, D. N. Neshev, W. Krolikowski, A. Arie, K. Koynov, and Y. S. Kivshar, "Cerenkov-type second-harmonic generation in two-dimensional nonlinear photonic structures," IEEE J. Quantum Electron. **45**, 1465 (2009).
15. M. Ayoub, P. Roedig, J. Imbrock, and C. Denz, "Cascaded Čerenkov third-harmonic generation in random quadratic media," Appl. Phys. Lett. **99**, 241109 (2011).
16. P. Tien, R. Ulrich, and R. Martin, "optical second harmonic generation in form of coherent cerenkov radiation from a thin-film waveguide," Appl. Phys. Lett. **17**, 447 (1970).
17. M.-J. Li, M. De Micheli, Q. He, and D. Ostrowsky, "Cerenkov configuration second harmonic generation in proton-exchanged lithium niobate guides," IEEE. J. Quantum Electron. **26**, 1384 (1990).
18. Y. Sheng, V. Roppo, K. Kalinowski, and W. Krolikowski, "Role of a localized modulation of χ (2) in Čerenkov second-harmonic generation in nonlinear bulk medium," Opt. Lett. **37**, 3864 (2012).
19. H. Ren, X. Deng, Y. Zheng, N. An, and X. Chen, "Enhanced nonlinear Cherenkov radiation on the crystal boundary," Opt. Lett. **38**, 1993 (2013).
20. R. W. Boyd, *Nonlinear Optics* (Academic, 2003).
21. Y. Sheng, Q. Kong, V. Roppo, K. Kalinowski, Q. Wang, C. Cojocaru, and W. Krolikowski, "Theoretical study of Čerenkov-type second-harmonic generation in periodically poled ferroelectric crystals," J Opt. Soc. Am. B **29**, 312 (2012).
22. A. Sugiyama, H. Fukuyama, T. Sasuga, T. Arisawa, and H. Takuma, "Direct bonding of Ti: sapphire laser crystals," Appl. Opt. **37**, 12 (1998).

1. Introduction

Nonlinear Cherenkov radiation (NCR) [1], an extension of the Cherenkov radiation well known in particle physics to nonlinear optics, has attracted considerable interest in recent years. In NCR, when the phase velocity of the fundamental wave (FW) exceeds that of the second harmonic (SH) wave, the SH radiates at an angle $\theta = arccos(v_2/v_1)$, where v_1 and v_2 denote the phase velocities of the FW and SH, respectively. This angle is determined by the dispersion relation of the nonlinear crystal and generally requires the crystal to be normally dispersive. Previous studies demonstrated that, under anomalous-like dispersion conditions, NCR can also be generated by modulating the phase velocity of the polarization wave [2]. NCR has been thoroughly researched in different nonlinear processes, such as second [3] and cascaded high-order harmonic generation [4–6], sum-frequency generation [7], and difference-frequency generation [8]. Such studies suggest potential applications to efficient frequency conversion [9], terahertz wave generation [10], ultrashort pulse-sharping [11], non-destructive domain-wall detection and imaging [12, 13], and so on.

Generally, efficient NCR occurs in nonlinear crystals with a random domain structure and in artificial periodic domain reversed structures [14, 15], as well as waveguide structures [16, 17]. The domain wall, which is the interface between antiparallel domains, modulates the second-order nonlinear coefficient $\chi^{(2)}$ from 1 to -1. As NCR is a longitudinal auto-phase-matched process, domain structures can provide reciprocal vectors to compensate the phase mismatching in the transverse direction. Recent theoretical [18] and experimental [19] studies showed that NCR can be enhanced at crystal boundaries by a sharp spatial modulation of $\chi^{(2)}$ from 1 to 0. However, for some nonlinear media, especially UV-transparent crystals, the intensity of NCR generated at the boundary is not very high since the nonlinear coefficient is comparatively small. The scenario where NCR is generated at an interface between two different quadratic crystals, where $\chi^{(2)}$ modulates from C_1 to C_2 (constants), has not been fully discussed. Theoretically, if the vacuum on the one side of the boundary is substituted by a nonlinear crystal with a much higher $\chi^{(2)}$ than the other, NCR is expected to be enhanced at the interface, as a result of the sharp $\chi^{(2)}$ modulation.

In this letter, we fabricated a structure where two crystals with different nonlinear coefficients are tightly abutted upon each other, We then demonstrated, both theoretically and experimentally, that NCR in a bulk medium can be enhanced by the presence of another medium. As the

#263353 Received 19 Apr 2016; revised 26 May 2016; accepted 30 May 2016; published 3 Jun 2016

radiation angle is determined by the dispersion relationship of the medium, the added crystal does not change the NCR properties. We observed a four- to tenfold enhancement of NCR under normal dispersion conditions. In an anomalous dispersion environment, enhanced NCR was also recorded.

2. The coupled wave equation and simulation

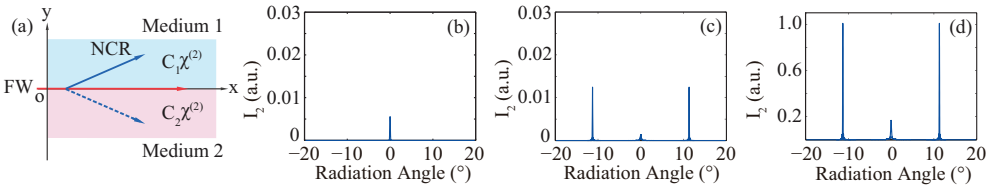

Fig. 1. NCR Simulation at an interface. (a) Structure of a nonlinear medium. The $y = 0$ plane is the interface between media 1 and 2, which have different second nonlinear coefficients $C_1\chi^{(2)}$ and $C_2\chi^{(2)}$, respectively. The FW is incident along the x axis. (b), (c) and (d) are the simulation results under the conditions $C_1 = 1$, $C_2 = 1$; $C_1 = 1$, $C_2 = 0$; $C_1 = 1$, $C_2 = 10$, respectively.

To analyze the second harmonic (SH) generated at the nonlinear interface, we consider two semi-infinite media with different second-order nonlinear coefficients $C_1\chi^{(2)}$ and $C_2\chi^{(2)}$, as in Fig. 1(a). For simplicity, the refractive index is assumed to be homogenous. The FW incident along the x axis is a Gaussian beam with width a. Considering the slowly varying envelope approximation, the coupled wave equation of SH is [20, 21]:

$$(\frac{\partial}{\partial x} + \frac{i}{2k_2}\frac{\partial^2}{\partial y^2})A_2(x,y) = -i\frac{k_2}{2n_2^2}g(y)\chi^{(2)}(A_1e^{-y^2/a^2})^2e^{i\Delta kx}, \tag{1}$$

where n_2 is the refractive index of the SH, A_1 and A_2 denote the complex amplitudes of the FW and SH, respectively. The phase mis-matching is $\Delta k = k_2 - 2k_1$, where k_1 and k_2 are the wave vectors of the FW and SH, and $g(y)$ is the spatial modulation function of $\chi^{(2)}$ along the y axis:

$$g(y) = \begin{cases} C_1 & y \geq 0 \\ C_2 & y < 0. \end{cases} \tag{2}$$

The FW amplitude is assumed to be constant. Using the Fourier transform, we can solve the coupled wave equation, and the intensity of SH $I_2(x,k_y) = |A_2(x,k_y)|^2$ can then be expressed as:

$$\begin{aligned} I_2(x,k_y) = &\Big[\frac{k_2}{2n_2^2}\chi^{(2)}\Big]^2 I_1^2x^2sinc^2\Big[\frac{(\Delta k - k_y/2k_2)x}{2}\Big] \\ &\Big|(C_1+C_2)\sqrt{\frac{\pi}{8}}ae^{-\frac{a^2k_y^2}{8}} + i(C_1-C_2)\frac{\sqrt{\pi}}{2}aD\big(\frac{ak_y}{2\sqrt{2}}\big)\Big|^2, \end{aligned} \tag{3}$$

where $k_y = k_2 sin\theta$ is the transverse wave vector of the SH, θ is the radiation angle, and $D\big(\frac{ak_y}{2\sqrt{2}}\big)$ denotes the Dawson function.

Equation (3), indicates that, when $C_1 - C_2 = 0$, the SH intensity I_2 gathers in the direction defined by $k_y = 0$, since $e^{-a^2k_y^2/8}$ decreases sharply with increasing k_y. When $C_1 - C_2 \neq 0$, the radiation angle of the SH is determined by the term containing $sinc^2[(\Delta k - k_y/2k_2)x/2]$.

#263353 Received 19 Apr 2016; revised 26 May 2016; accepted 30 May 2016; published 3 Jun 2016

The solution of $\Delta k - k_y/2k_2 = 0$ is $k_y^2 = k_2^2 - (2k_1)^2$, assuming $k_y^2 \ll k_2^2$. From the geometrical relationship, we can deduce the radiation angle satisfying $k_2 cos\theta = 2k_1$, which is exactly the longitudinal phase-matching condition of NCR. Nonlinearity enhancement can be attributed mainly to the term of $C_1 - C_2$, whose absolute value is directly proportional to the SH intensity, according to Eq. (3). The SH intensity depends on the sharp change of $\chi^{(2)}$, i.e., if the absolute value of $C_1 - C_2$ increases, the NCR intensity is enhanced.

The simulation results for different parameters are depicted in Figs. 1(b)–1(d). The FW wavelength is 800 nm. Both the FW and NCR are o-polarized. The interaction length is 200 μm. Since we are concerned about the spatial modulation of $\chi^{(2)}$ at the medium interface, other properties of media 1 and 2 are supposed to be the same in the simulation. For simplicity and without loss of generality, the dispersion of a $\beta - BaB_2O_4$ crystal (BBO) is assumed for the media on both sides of the interface, unless otherwise stated. The simplest situation is to consider a whole bulk medium where $C_1 = C_2$. The result is a general phase-mismatched SH generation, with an extremely weak SH output that is collinear with the FW at zero angle, as shown in Fig. 1(b). In Fig. 1(c), the modulation function of $\chi^{(2)}$ changes from 1 to 0. It describes NCR at the boundary of a nonlinear crystal. The radiation angle of the efficient SH is $\pm 11.28^\circ$, as is the calculated Cherenkov angle in BBO. Figure 1(d) shows the simulation result in agreement with our analysis where $C_1 = 1$, $C_2 = 10$. The NCR intensity is a hundred times that in Fig. 1(c). Notably, the NCR radiation angle is the same as that in Fig. 1(c) since it depends solely on the dispersion relationship between the SH and FW.

3. Experiment results and discussion

In the experiment, two different nonlinear crystals tightly abutted upon each other under high pressure were used to achieve a sharp modulation of $\chi^{(2)}$. For Sample 1, as shown in Fig. 2(a), we chose a z-cut BBO crystal of size 5 mm(x)×10 mm(y)×10 mm(z) and a y-cut 5 mol% MgO : $LiNbO_3$ (LN) crystal of size 10 mm(x)×10 mm(y)×5 mm(z). The nonlinear coefficient of LN is much greater than that of BBO. And the orientation of the nonlinearity effects the polarization direction of nonlinear polarization wave and further determines the polarization direction of NCR. If the FW is o-polarized, the effective second-order nonlinear coefficient is d_{11} in BBO, and d_{33} in LN, and the absolute value of $C_1 - C_2$ is about 14 [20]. For Sample 2 [Fig. 2(b)], the orientation of the LN crystal was changed to z-cut and its size was 5 mm(x)×10 mm(y)×10 mm(z). If the nonlinear process is oo-e, the effective second-order nonlinear coefficients in BBO and LN are both d_{31}, and the absolute value of $C_1 - C_2$ is about 48.

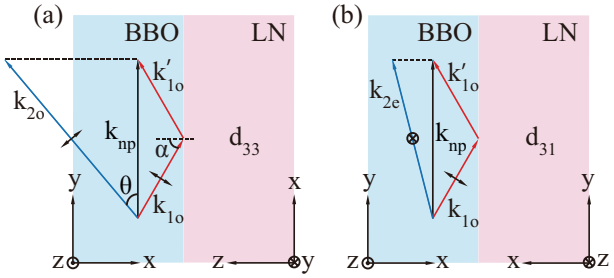

Fig. 2. Schematic experimental samples viewed from the top. (a) Sample 1: z-cut BBO and y-cut LN. (b) Sample 2: z-cut BBO and z-cut LN.

The phase-matching geometries in both scenarios are shown in Fig. 2. Since the two crystals are just pressed together, there is an air gap with a thickness of about several micron. The FW is incident from BBO to LN with an incident angle of α with respect to the interface. Reflection

#263353 Received 19 Apr 2016; revised 26 May 2016; accepted 30 May 2016; published 3 Jun 2016

and refraction of the FW occur as a result of the refractive-index inhomogeneity. However this does not qualitatively affect NCR generation at the nonlinear interface emitting into the BBO side. The nonlinear polarization wave, stimulated by the obliquely incident FW, propagates along the interface. Its wave vector is $k_{np} = 2k_1 sin\alpha$. When exceeding the threshold ($k_{np} \leq k_2$), Cherenkov radiation is emitted at an angle $\theta = arccos(k_{np}/k_2)$. This remains unchanged, regardless of the presence of LN on the other side.

Figure 3(a) shows a schematic of our experiment. The FW was provided by a regenerative amplifier delivering 50 -fs pulses at a 1 -kHz repetition rate with a wavelength centering at 800 nm and an average power of 4.0 mW. The FW was loosely focused by a 100 -mm focal-length lens to a beam waist of 50 μm. The beam was obliquely incident onto BBO crystal and reflected at the BBO-LN interface. The output light was then projected onto a screen.

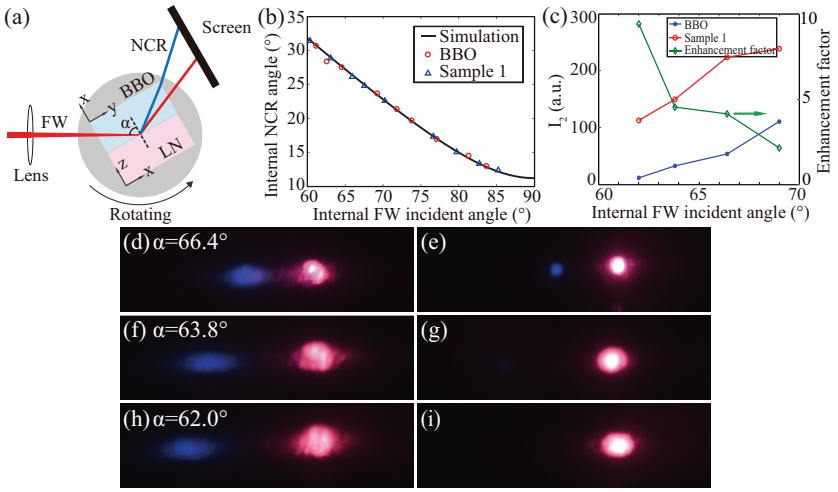

Fig. 3. (a) Schematic experimental setup. (b) Internal NCR angle θ under normal dispersion versus FW incident angle α. Theoretical prediction (solid curve) and experimental results (symbols) are in good agreement. (c) Measured intensity and enhancement factor of SH generated at the BBO-LN interface and boundary of BBO crystal. (d), (f) and (h) are the recorded patterns with varying FW incident angle at the BBO-LN interface. (e), (g) and (i) are the recorded patterns of the FW incident on the BBO crystal boundary with the same angle as in (d), (f) and (h), respectively.

Sample 1 was first illuminated by the o-polarized FW. By turning the incident angle α, o-polarized second harmonic wave could be observed at different radiation angles. This is NCR in a normal dispersion environment, displayed as an oo-o nonlinear process in BBO. We measured the internal NCR angle θ as a function of the FW incident angle α. The theoretical prediction and experimental results are in good agreement, as shown in Fig. 3(b). Both at the boundary of the single BBO crystal and at the interface of Sample 1, the relationship between θ and α depends solely on the BBO dispersion.

The recorded patterns with different FW incident angles 66.4°, 63.8°, and 62.0° are presented in Figs. 3(d), 3(f), and 3(h), respectively. For comparison, the NCR generated at the boundary of the single BBO crystal was also observed [see Figs. 3(e), 3(g), and 3(i)]. Obviously, at the same FW reflection angle, the intensity of NCR generated at the interface of Sample 1 was much higher than that generated at the BBO boundary. This observation verifies the preceding simulation result that NCR is enhanced at an interface where the modulation of $\chi^{(2)}$ is sufficiently large. The enhancement factor ranges from approximately 4 [Fig. 3(d)] to 10 [Fig. 3(h)]

#263353 Received 19 Apr 2016; revised 26 May 2016; accepted 30 May 2016; published 3 Jun 2016

and varies with the FW reflection angle [Fig. 3(c)]. The quality of the interface, and the partial reflection of the FW from it, degrade the conversion efficiency as the two crystals are simply pressed together to form the interface and an air gap between them is unavoidable. Using diffusion bonding [22] or other direct bonding techniques, the interface of the two nonlinear materials may be much smoothed and the NCR intensity can be further enhanced.

Sample 2 was used to repeat the experiment. Compared with Sample 1, the o-polarized NCR was not enhanced because of the absence of d_{11} in LN. However, an e-polarized SH can be observed if the incident angle α is smaller than 70° [Figs. 4(b)-4(e)]. This oo-e process occurs under anomalous-like dispersion conditions, considering the refractive index of BBO. When the SH wave vector $k_{2e} \geq 2k_{1o}sin\alpha$, the NCR condition is satisfied. The experiment results and theoretical prediction are also in good agreement [Fig. 4(a)]. This phenomenon was not observed in Sample 1 or in single BBO, because d_{31} is much smaller than d_{11} in BBO and the d_{13} of LN is zero. In an anomalous-like dispersion environment, the SH intensity may be further enhanced by using other crystals with a high nonlinear coefficient.

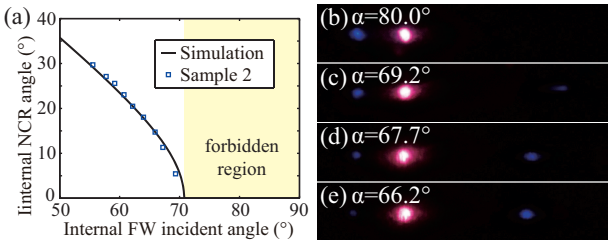

Fig. 4. (a) The internal NCR angle θ under anomalous dispersion versus the incident angle of FW α. (b)-(e) are the recorded patterns varying with the incident angle of FW.

The advantage of this method is that another material can be used to enhance the nonlinear process in the crystal of interest, without changing its properties. For example, in an LN crystal, light with wavelength below 380 nm is absorbed, but can be used to enhance ultraviolet SH generation in BBO. Our scheme may provide a new way for practical applications to ultraviolet laser sources and efficient nonlinear processes.

4. Conclusion

In summary, we demonstrated both theoretically and experimentally, that NCR generation can be enhanced at the nonlinear interface of two different nonlinear materials. The sharper the change in nonlinear coefficient, the higher the NCR intensity. Under normal dispersion conditions, the NCR generated at a BBO-LN interface is enhanced by a factor in the range of 4 to 10, compared with that at the boundary of a single BBO crystal. Under anomalous dispersion conditions, an oo-e type of NCR was observed as a result of the enhancement at the nonlinear interface. The added nonlinear material does not change the properties of the Cherenkov radiation, such as the emission angle.

Acknowledgments

This work was supported in part by the National Basic Research Program 973 of China under Grant No.2011CB808101, the National Natural Science Foundation of China under Grant Nos. 61125503, 61235009, 61205110 and 61505189, the Foundation for Development of Science and Technology of Shanghai under Grant No. 13JC1408300, the Innovative Foundation of Laser Fusion Research Center, and in part by the Presidential Foundation of the China Academy of Engineering Physics (Grant No.201501023).

#263353 Received 19 Apr 2016; revised 26 May 2016; accepted 30 May 2016; published 3 Jun 2016